CRYO/02/028
April 5, 2002

Inductance Calculation for Conductors of Arbitrary Shape

L. Bottura

Distribution: Internal

Summary

In this note we describe a method for the numerical calculation of inductances among conductors of arbitrary shape. The conductor is discretized using isoparametric bricks with uniform current density. The calculation is numerically stable and automatically adaptive up to a predefined accuracy. A convergence acceleration based on the study of the numerical error properties is used to achieve fast and accurate results.

1. Introduction

In the electromagnetic analysis of magnetic configurations, in circuital analysis and in general in electrical engineering it is often necessary to have a precise value of the self and mutual indutance of conductors. In the case of simple configurations the inductance calculation is often performed using analytical approximations. Once the configuration becomes complex, or tends to limits of small distances or small conductor size, analytical approximation can become very inaccurate, and in the limit fail to provide physically consistent values. In this note we describe a numerical method suitable for aritrary, three-dimensional conductor shape that gives accurate results in all limiting cases.

For the calculation of the inductance we start from the following expression of the magnetic energy E_{ij} stored in the interaction of the current flowing in two conductors i and j of arbitrary shape and volume V_i and V_j:

$$E_{ij} = \frac{1}{2}\frac{\mu_0}{4\pi}\iint_{Vi\,Vj}\frac{\mathbf{J}_i \bullet \mathbf{J}_j}{|\mathbf{r}_{PQ}|}dV_j dV_i \tag{1.1}$$

where $\mathbf{J}_i$ is the current density in the volume V_i, $\mathbf{J}_j$ is the current density in the volume V_j and $\mathbf{r}_{PQ}$ is the vector distance between a point Q centered in the

volume element dV_j, and a point P centered in the volume element dV_i. We show this situation in Fig. 1 for the case of two conductors of arbitrary shape and position in space.

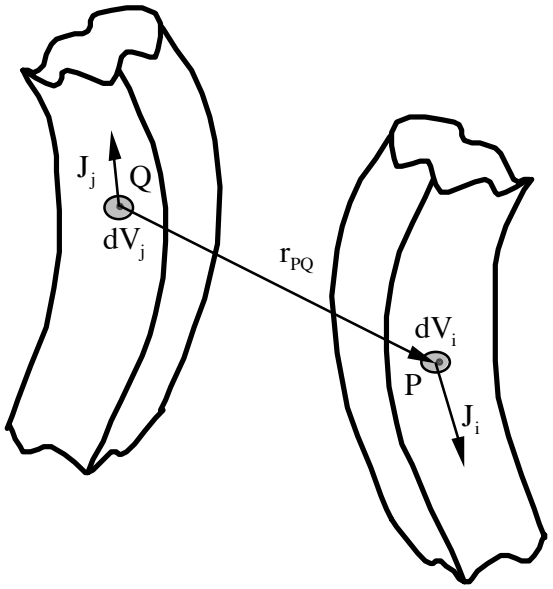

Figure 1. Definition for the calculation of inductance coefficients among conductors of arbitrary shape.

Note that E_{ij} is only the portion of magnetic energy associated with the interaction of conductors i and j. The total magnetic energy E stored in the system can be obtained by the sum:

$$E = E_{ii} + E_{ij} + E_{ji} + E_{jj} \tag{1.2}$$

where all possible interactions must be considered. In the absence of current sources or sinks, each conductor carries a total current I_i and I_j constant along its length, and the corresponding interaction energy can be also written using the inductance L_{ij} as follows:

$$E = \frac{1}{2} L_{ij} I_i I_j \tag{1.3}$$

We define now two versors $\mathbf{j}_i$ and $\mathbf{j}_j$ oriented as the current density in the conductors, but with module normalised to provide unit current in the conductor. The current density in the conductor i can then be written as:

$$\mathbf{J}_i = I_i \mathbf{j}_i \tag{1.4}$$

and similarly for the conductor *j*. With the above definition we can identify terms in Eqs. (1.1) and (1.3) to obtain:

$$L_{ij} = \frac{\mu_0}{4\pi} \iint_{Vi\,Vj} \frac{\mathbf{j}_i \bullet \mathbf{j}_j}{|\mathbf{r}_{PQ}|} dV_j dV_i \tag{1.5}$$

The order of the scalar product and integration in Eq. (1.5) can be changed as follows:

$$L_{ij} = \frac{\mu_0}{4\pi} \int_{Vi} \mathbf{j}_i \bullet \left(\int_{Vj} \frac{\mathbf{j}_j}{|\mathbf{r}_{PQ}|} dV_j \right) dV_i \tag{1.6}$$

where we recognize that the product of the multiplicative constant and of the term in parantheses corresponds by definition to the vector potential $\mathbf{A}_j$ generated by a current density of strength $\mathbf{j}_j$ in the conductor *j*, or:

$$\mathbf{A}_j = \frac{\mu_0}{4\pi} \int_{Vj} \frac{\mathbf{j}_j}{|\mathbf{r}_{PQ}|} dV_j \tag{1.7}$$

Accordingly, the inductance coefficient can also be written as follows:

$$L_{ij} = \int_{Vi} \mathbf{j}_i \bullet \mathbf{A}_j dV_i \tag{1.8}$$

In the above form the inductance calculation can therefore be reduced to the volume integral in conductor *i* of the scalar product of the current density versor $\mathbf{j}_i$ and the vector potential $\mathbf{A}_j$ generated by a current density of strength $\mathbf{j}_j$ in the conductor *j*. This form is the most convenient for numerical integration.

2. Numerical calculation

2.1 Discretization

For the numerical integration of Eq. (1.8) we start discretising the system of conductors using 8-nodes brick elements with plane faces. The integral of the scalar quantity, the product $\mathbf{j}_i \bullet \mathbf{A}_j$, over the volume V_i of conductor *i* is then broken into the sum of the integrals over its N_i elements of volume V_{Ni}:

$$L_{ij} = \int_{Vi} \mathbf{j}_i \bullet \mathbf{A}_j dV_i = \sum_{Ni} \int_{V_{Ni}} \mathbf{j}_i \bullet \mathbf{A}_j dV_{Ni} \tag{2.1}$$

To perform the volume integration in each element of conductor *i* we need the value of the vector potential generated at an arbitrary point by the elements belonging to conductor *j*. For this calculation we use the analytic expressions established in [2]. As explained there, the calculation is performed transforming the volume integral in a sum of line integrals over the edges of the isoparametric brick, and is exact in the case that the faces of the brick are plane.

The integral over the volume V_{Ni} is performed numerically using Gauss quadrature [3]. To this aim we use the coordinate transformation properties of an isoparametric element to transform the volume integral in Eq. (2.1) as follows:

$$\int_{V_{Ni}} \mathbf{j}_i \bullet \mathbf{A}_j dV_{Ni} = \int_{-1}^{1}\int_{-1}^{1}\int_{-1}^{1} (\mathbf{j}_i \bullet \mathbf{A}_j) D d\xi d\eta d\zeta \tag{2.2}$$

where the integration is transformed from the volume V_{Ni} of the element in physical space to the right prism with vertices placed at coordinates +1 and -1 in the parent space (ξ,η,ζ) as shown in Fig. 2. The transformation is defined as conventionally done in finite element theory using the determinant D of the Jacobian matrix[3].

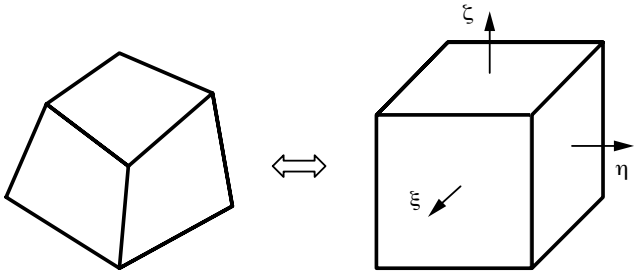

Figure 2. Transformation of an isoparametric brick in physical space to the right prism in the parent space.

The numerical integration of Eq. (2.2) is simplified by the fact that it takes place in the parent plane, where the integration interval is [-1…1]. For the integration in 3-D space we use the same number N of Gauss points with coordinates $\xi_k = \eta_l = \zeta_m$ and associated weight w in the three directions and we can write the integral as follows:

$$\int_{-1}^{1}\int_{-1}^{1}\int_{-1}^{1} (\mathbf{j}_i \bullet \mathbf{A}_j) D d\xi d\eta d\zeta \approx \sum_{k=1}^{N}\sum_{l=1}^{N}\sum_{m=1}^{N} w_k w_l w_m (\mathbf{j}_i \bullet \mathbf{A}_j(\xi_k,\eta_l,\zeta_m)) D(\xi_k,\eta_l,\zeta_m) \tag{2.3}$$

where we have evidenced the fact that the current density is constant while the vector potential and the Jacobian must be evaluated at each Gauss point.

2.2 *Convergence acceleration and adaptivity*

The sum on the r.h.s. of Eq. (2.3) provides an approximation u to the exact integral u_{exact} over each element. The quality of the approximation improves, and the associated error $\varepsilon = u - u_{exact}$ decreases, increasing the number of Gauss points used for the evaluation, i.e. the *order* of the integration. In general we can write that the result of the integral is affected by an error that depends asymptotically on the integration order as follows:

$$\varepsilon = C\left(\frac{1}{N}\right)^R \tag{2.4}$$

where C is a constant and R is the convergence rate of the numerical approximation. Provided that the relation Eq. (2.4) holds, it is possible to use the result of the numerical integral obtained using different integration orders to estimate the integration error and thus improve the result. We refer to this process as *convergence acceleration*. Assuming in particualr that the numerical integral has been performed for two different orders N and N-1, leading to the two results u_N and $u_{N\text{-}1}$ respectively, we can calculate the multiplicative constant C:

$$C = \frac{u_N - u_{N-1}}{\left(\frac{1}{N}\right)^R - \left(\frac{1}{N-1}\right)^R} \tag{2.5}.$$

The asymptotic value of the integral for an infinite integration order is then estimated as follows from the result obtained using an integration order N:

$$u_N^\infty \approx u_N - C\left(\frac{1}{N}\right)^R \tag{2.6}.$$

The estimate thus obtained for the integration order N can be compared to a previous estimate, obtained for an order M with $M < N$ to verify the convergence by computing the variation δ among the two estimates:

$$\delta \approx 2\frac{\left|u_N^\infty - u_M^\infty\right|}{\left|u_N^\infty\right| + \left|u_M^\infty\right|} \tag{2.7}.$$

The parameter δ provides a simple mean to adapt the integration order. The integration is started with a single Gauss point, i.e. N=1. The order is augmented, recomputing at each successive integration the estimate u_N^∞ and monitoring the variation δ between successive integrations (i.e. $M = N$-1). Convergence is achieved when the variation δ becomes smaller than a pre-set value.

The procedure outline here requires the knowledge of the convergence rate R, discussed in the next section.

2.3 Convergence rate

In order to determine the conmvergence rate R to be used in the adaptive procedure described, we have performed tests of inductance calculations on brick elements placed differently in space. The first test was performed using as conductors right prisms of size 2 m placed as shown in Figure 3(a). The current was assumed to flow along the z axis of the prisms. The second convergence test was performed on the bricks used to discretized two co-axial solenoids of inner radius 0.5 m, outer radius 1.5 m and height 1 m and placed as shown in Fig. 3(b). The solenoids were discretized using 50 isoparametric bricks each.

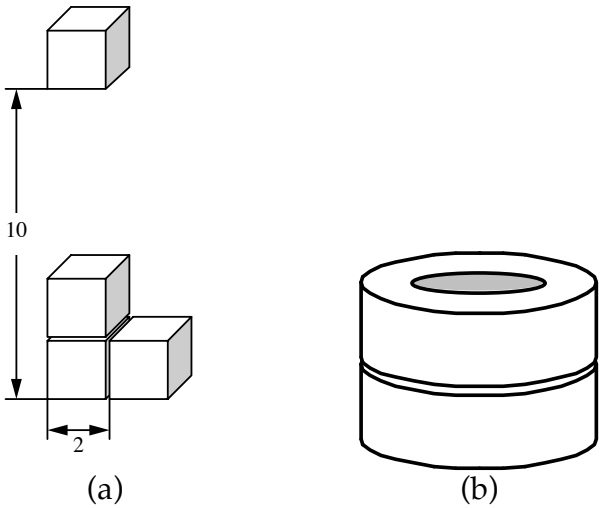

Figure 3. Geometry used for the convergence tests.

Calculations of the self and mutual inductance of the bricks were performed using 1 to 10 Gauss points in each space direction. The error ε was computed assuming that the *exact* value of the integral u_{exact} is the asymptotic value u_N^∞ estimated for the highest integration order (i.e. N = 10). In addition we have computed the error on the asymptotic estimate ε^∞ given by the difference between the asymptotic value u_N^∞ at a given order N and the exact value u_{exact}, i.e. $\varepsilon^\infty = u_N^\infty - u_{exact}$. In Figs. 4 and 5 we report the results of this analysis. The errors

have been normalised to the exact solution, and are plotted in absolute value. We see that for both calculations that the relative error on the computed inductances of closely placed bricks is at the ppm level for an integration of order 6 and higher. For bricks with large spacing compared to the dimensions the required integration order to reach ppm accuracy is much smaller, and typically 2 to 3 Gauss points per direction are enough. The typical convergence rate R is of the order of 7.5.

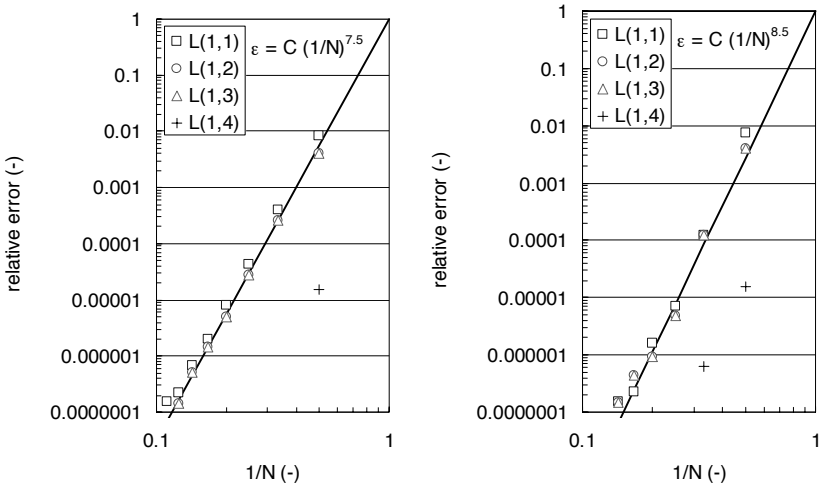

Figure 4. Convergence rate of the computed self and mutual inductance coefficients for the first test case (right prisms). On the left the relative error on the volume given by Eq. (2.3), on the right the relative error on the asymptotic estimate provided by Eq. (2.6). In both cases the power law is plotted for C=1.

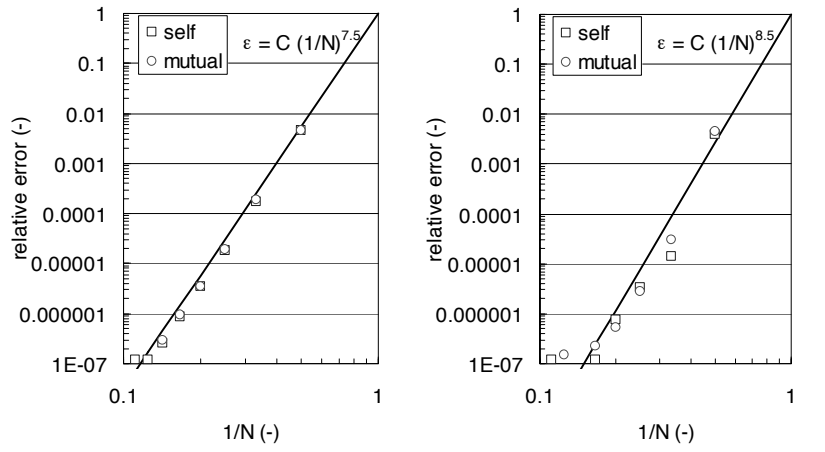

Figure 5. Convergence rate of the computed self and mutual inductance coefficients for the second test case (co-axial solenoids). On the left the relative error on the volume given by Eq. (2.3), on the right the relative error on the asymptotic estimate provided by Eq. (2.6). In both cases the power law is plotted for C=1.

The asymptotic estimate of the integrals converges faster, typically with a rate $(R + 1)$ and higher. The gain in the convergence rate allows to reach higher accuracy for a given integration order or the same accuracy with a reduced order. This prooves that the acceleration procedure devised works as expected.

3. *Example*

As a final test of the procedure described here we have tested the convergence of the calculation of the inductance of the solenoid configuration reported in Fig. 3(b) and we have compared it to known analytical solutions. The self inductance of each solenoid computed with the analytical approximations given in [4] is 1.2666 μH, while the mutual inductance is 0.5457 μH. The numerical calculation was performed for a discretization of the first solenoid using 100 bricks, while for the second a variable number of bricks in the range of 5 to 80 has been used in order to establish the convergence rate. The result for the largest number of bricks is a self inductance of 1.2655 μH and a mutual inductance of 0.5397 μH. Both values agree well with the analytical approximations quoted above.

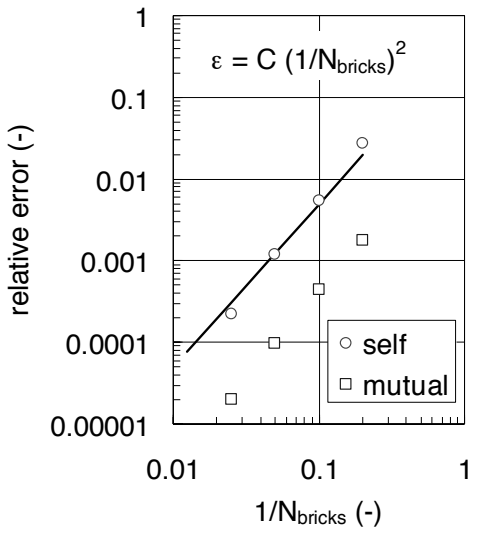

Figure 5. Convergence of the calculation of self and mutual inductance for a set of two co-axial solenoids. The power law is plotted for C=0.5.

The convergence of self and mutual inductance calculation is shown in Fig. 6. In this case the convergence appears to be quadratic. The reason for the apparent loss of convergence speed is that in this test an additional error is generated by the approximation of the solenoid geometry through bricks. The curved geometry is approximated better at increasing number of bricks, and it can be shown that the geometrical error of this approximation process has a quadratic convergence. This error dominates the overall performance of the calculation, thus hiding the higher convergence rate that is achieved on a brick-by-brick

basis. It is therefore clear that care should be exerted when approximating curved geometries with bricks and in estimating the associated error. In spite of this the calculation achieves remarkable accuracy with moderate number of bricks.

References

[1] F. Barozzi, F. Gasparini, *Fondamenti di Elettrotecnica*, UTET, 1989.

[2] L. Bottura, *Analytical Calculation of Vector Potential in an Isoparametric Brick*, CryoSoft Internal Note CRYO/97/003, 1997.

[3] O.C. Zienkiewicz, *The Finite Element Method*, 4th Edition, McGraw Hill, 1991

[4] F.W. Grover, *Inductance Calculations*, Dover Publications, 1946.